J|A|C|S
ARTICLES
Published on Web 01/31/2002

Modeling the Active Site of Cytochrome Oxidase: Synthesis and Characterization of a Cross-Linked Histidine−Phenol

Jenny A. Cappuccio,[†] Idelisa Ayala,[‡] Gregory I. Elliott,[†] Istvan Szundi,[†] James Lewis,[†] Joseph P. Konopelski,[†] Bridgette A. Barry,[‡] and Ólöf Einarsdóttir*[,†]

Contribution from the Department of Chemistry and Biochemistry, University of California Santa Cruz, California 95064, and Department of Biochemistry, Molecular Biology, and Biophysics, University of Minnesota, 1479 Gortner Avenue, St. Paul, Minnesota 55108

Received July 30, 2001

Abstract: A cross-linked histidine−phenol compound was synthesized as a chemical analogue of the active site of cytochrome *c* oxidase. The structure of the cross-linked compound (compound **1**) was verified by IR, ^{1}H and ^{13}C NMR, mass spectrometry, and single-crystal X-ray analysis. Spectrophotometric titrations indicated that the pK_a of the phenolic proton on compound **1** (8.34) was lower than the pK_a of tyrosine (10.1) or of *p*-cresol (10.2). This decrease in pK_a is consistent with the hypothesis that a cross-linked histidine−tyrosine may facilitate proton delivery to the binuclear site in cytochrome *c* oxidase. Time-resolved optical absorption spectra of compound **1** at room temperature, generated by excitation at 266 nm in the presence and absence of dioxygen, indicated a species with absorption maxima at ∼330 and ∼500 nm, which we assign to the phenoxyl radical of compound **1**. The electron paramagnetic resonance (EPR) spectra of compound **1**, obtained after UV photolysis, confirmed the generation of a paramagnetic species at low temperature. Because the cross-linked compound lacks β-methylene protons, the EPR line shape was dramatically altered when compared to that of the tyrosyl radical. However, simulation of the EPR line shape and measurement of the isotropic *g* value was consistent with a small coupling to the imidazole nitrogen and with little spin density perturbation in the phenoxyl ring. The ground-state Fourier transform infrared (FT-IR) spectrum of compound **1** showed that addition of the imidazole ring perturbs the frequency of the tyrosine ring stretching vibrations. The difference FT-IR spectrum, associated with the oxidation of the cross-linked compound, detected significant perturbations of the phenoxyl radical vibrational bands. We postulate that phenol oxidation produces a small delocalization of spin density onto the imidazole nitrogen of compound **1**, which may explain its unique optical spectral properties.

Introduction

Cytochrome *c* oxidase, the terminal protein in the electron transport chain, catalyzes the sequential four-electron transfer from cytochrome *c* to dioxygen.[1] The reduction of dioxygen to water is coupled to the translocation of four protons across the inner mitochondrial membrane (or the bacterial cytoplasmic membrane).[2] The resulting electrochemical proton gradient is used by ATP synthase to generate ATP. The O_2 reduction takes place at the heme a_3/Cu_B binuclear site. Recent X-ray crystallographic studies on the bovine heart[3] and *Paracoccus denitrificans*[4] cytochrome oxidases have shown that the active site contains an unprecedented cross-link between C6 of a tyrosine residue (Tyr244) and the ϵ-nitrogen of histidine 240, which is a ligand to Cu_B.

The details of the mechanism of the reduction of dioxygen to water are still unresolved. A "peroxy" intermediate (P) has been proposed following the binding of O_2 to heme a_3. While previous studies proposed that the O−O bond in P was intact, more recent studies showed that the O−O bond is already broken and that P is in fact an oxyferryl state, $Fe_{a3}^{4+}{=}O^{2-}$.[5−8] The discovery of the tyrosine−histidine cross-link at the active site led to the proposal that the tyrosine may function as an electron[9] and a proton donor to the dioxygen bound to heme a_3,[7,10,11] thus facilitating the cleavage of the dioxygen bond. One of the protons taken up by cytochrome oxidase upon reduction

* To whom correspondence should be addressed. E-mail: olof@chemistry.ucsc.edu. Fax: 831-459-2935.
[†] University of California Santa Cruz.
[‡] University of Minnesota.

(1) Ferguson-Miller, S.; Babcock, G. T. *Chem. Rev.* **1996**, *96*, 2889−2907.
(2) Wikström, M. K. F. *Nature* **1977**, *266*, 271−273.
(3) Yoshikawa, S.; Shinzawa-Itoh, K.; Nakashima, R.; Yaone, R.; Yamashita, E.; Inoue, N.; Yao, M.; Fei, M. J.; Libeu, C. P.; Mitzushima, T.; Yamaguchi, H.; Tomizaki, T.; Tsukihara, T. *Science* **1998**, *280*, 1723−1731.
(4) Ostermeier, C.; Harrenga, A.; Ermler, U.; Michel, H. *Proc. Natl. Acad. Sci. U.S.A.* **1997**, *94*, 10547−10553.
(5) Proshlyakov, D. A.; Ogura, T.; Shinzawa-Itoh, K.; Yoshikawa, S.; Appelman, E. H.; Kitagawa, T. *J. Biol. Chem.* **1994**, *269*, 29385−29388.
(6) Proshlyakov, D. A.; Ogura, T.; Shinzawa-Itoh, K.; Yoshikawa, S.; Kitagawa, T. *Biochemistry* **1996**, *35*, 76−82.
(7) Proshlyakov, D. A.; Pressler, M. A.; Babcock, G. T. *Proc. Natl. Acad. Sci. U.S.A.* **1998**, *95*, 8020−8025.
(8) Fabian, M.; Wong, W. W.; Gennis, R. B.; Palmer, G. *Proc. Natl. Acad. Sci. U.S.A.* **1999**, *96*, 13114−13117.
(9) Blomberg, M. R. A.; Siegbahn, P. E. M.; Babcock, G. T.; Wikström, M. *J. Inorg. Biochem.* **2000**, *80*, 261−269.
(10) Gennis, R. B. *Biochim. Biophys. Acta* **1998**, *1365*, 241−248.
(11) Sucheta, A.; Szundi, I.; Einarsdóttir, O. *Biochemistry* **1998**, *37*, 17905−17914.

10.1021/ja011852h CCC: $22.00

of the binuclear center has been proposed to protonate the tyrosine, thereby preparing it for its role in the cleavage of the O−O bond.[10]

While recent experiments have provided support for the role of a tyrosyl radical in the P form of the enzyme,[7,12−14] direct evidence for the participation of the tyrosyl radical in the mechanism is lacking. The expected EPR signals from the $S = {}^1/_2$ $Cu_B{}^{2+}$ and $S = {}^1/_2$ Tyr244$^\bullet$ have not been detected in the P form of the bovine heart enzyme. This has been attributed to a possible spin coupling between the two species that is mediated by the ligated cross-linked His240.[7]

It is clear that further studies are needed to establish whether the cross-linked tyrosine plays a key role in the mechanism of the reduction of dioxygen to water by cytochrome oxidase. In particular, it is important to understand whether the cross-link between the histidine and tyrosine changes the properties of the tyrosine to facilitate its role in dioxygen reduction. Recent studies on 2-imidazol-1-yl-4-methylphenol have suggested that the cross-link will facilitate proton delivery to the binuclear center in the enzyme.[15] It is also of interest to determine whether the proposed radical resides on the tyrosine or the histidine. In this work, we present the synthesis and spectroscopic studies of a His−phenol cross-linked compound (compound **1**), a chemical analogue of the active site of cytochrome oxidase. Our spectrophotometric titrations show that the pK_a of the phenolic proton on the cross-linked compound is lowered compared to that of tyrosine or *p*-cresol. This is consistent with the cross-linked tyrosine facilitating proton delivery to the binuclear site in cytochrome *c* oxidase.[7,10,15] In addition, the presence of a UV-generated radical in compound **1** is investigated at room temperature by time-resolved UV−vis spectroscopy and confirmed at low temperature by electron paramagnetic resonance (EPR) and Fourier transform infrared (FT-IR) difference spectroscopy. The data are consistent with the radical residing primarily on the phenoxyl ring with a small delocalization of spin density onto the imidazole.

Materials and Methods

Reagents. 3-Aminotyrosine, *p*-cresol, and L-tyrosine were purchased from Sigma−Aldrich (St. Louis, MO). The H-His-Tyr-OH dipeptide was purchased from Bachem (King of Prussia, PA). ^{13}C(6)-Tyrosine ([*ring*-^{13}C(6)]-L-tyrosine) was purchased from Cambridge Isotope Laboratories (Andover, MA) and was 98−99% labeled.

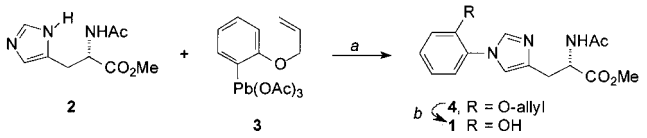

2 3

a) 10% $Cu(OAc)_2$, CH_2Cl_2, RT, 35%; *b)* $HSnBu_3$, 5% $PdCl_2(PPh)_2$, 99%

Synthesis of the His−Phenol Cross-Linked Compound: (A) 1-*o*-Allyoxyphenyl(acetyl)histidine Methyl Ester (4). *N*-α-Acetylhistidine methyl ester (**2**) (136 mg, 0.55 mmol) was stirred in 5 mL of dry CH_2Cl_2. To this suspension was added Cs_2CO_3 (195 mg, 0.6 mmol) along with $Cu(OAc)_2$ (12 mg, 0.077 mmol) and *o*-(prop-2-enyloxy)phenyllead triacetate (**3**) (400 mg, 0.77 mmol). The solution was allowed to stir at room temperature for 12 h, and the reaction was subsequently quenched with an aqueous solution of sodium sulfide. The black precipitate was filtered through Celite. The layers were separated and the aqueous layer was extracted with CH_2Cl_2. The organic layer was dried with $MgSO_4$ and purified by flash chromatography to provide (**4**) as a clear oil in 35% yield. $[\alpha]_D{}^{25}$ +6.8 (*c* 0.95, MeOH); ^{1}H NMR (500 MHz, $CDCl_3$) δ 7.706 (d, $J = 1$ Hz, 1H), 7.328 (dt, $J = 6.5$ Hz, 1H), 7.247 (d, $J = 7.5$ and 2 Hz, 2H), 7.041−6.993 (m, 2H), 6.001−5.924 (m, 1H), 5.338 (dq, $J = 17.5$ and 1.5 Hz, 1H), 5.269 (dq, $J = 10$ and 1 Hz, 1H), 4.868 (dt, $J = 7.5$ and 5 Hz, 1H), 4.567−4.524 (m, 2H), 3.693 (s, 3H), 3.196 (dq, $J = 57.5$, 14.5, and 5.5 Hz, 2H), 2.047 (s, 3H); ^{13}C NMR (125 Hz, $CDCl_3$) δ 172.1, 170.1, 151.5, 137.6, 137.1, 132.4, 128.9, 126.7, 125.5, 121.5, 118.0, 114.0, 69.7, 52.5, 52.3, 29.7, 23.3; IR (neat) 3246, 1721, 1669, 1245, 1003 cm^{-1}. HRMS Calcd for $[M]^+$ $C_{18}H_{21}N_3O_4$: 343.1532. Found: 343.1526.

(B) 1-*o*-Phenol(acetyl)histidine Methyl Ester (1). Tributyltin hydride (60 μL, 0.226 mmol) was slowly added to a solution of **4** (66 mg, 0.19 mmol) and bis(triphenylphosphine) palladium chloride (3 mg, 4.7 μmol) in 10 mL of dry tetrahydrofuran (THF). The solution darkens upon the final addition of tin hydride. The reaction mixture was allowed to stir at room temperature for 2 h and then concentrated in a vacuum to give an amber oil. Purification by flash chromatography provides the title compound (**1**) in 99% yield as a white solid. Material suitable for single-crystal X-ray analysis was obtained by recrystallization from MeOH: mp 201−203 °C; $[\alpha]_D{}^{25}$ +32.9 (*c* 1.35, MeOH); ^{1}H NMR (500 MHz, $CDCl_3$) δ 7.739 (d, $J = 1.5$ Hz, 1H), 7.239 (dt, $J = 8.5$ and 1.5 Hz, 1H), 7.190 (dd, $J = 13$ and 1.5 Hz., 1H), 7.099−7.052 (m, 3H), 6.931 (dt, $J = 8$ and 1.5 Hz, 1H), 4.833 (dq, $J = 6$ and 1.5 Hz, 1H), 3.674 (s, 3H), 3.098 (m, 2H), 1.965 (s, 3H); ^{1}H NMR (500 MHz, DMSO-d_6) δ 10.17 (br s, 1H), 8.238 (d, $J = 7.5$ Hz, 1H), 7.824 (s, 1H), 7.284 (dd, $J = 7.5$ and 1.5 Hz, 1H), 7.185 (m, 2H), 7.033 (dd, $J = 8.5$ and 1 Hz, 1H), 6.902 (dt, $J = 7$ and 1 Hz, 1H), 4.519 (q, $J = 8.5$ and 1 Hz, 1H), 3.601 (s, 3H), 2.942 (dq, $J = 14$ and 8 Hz, 2H), 1.822 (s, 3H); ^{13}C NMR (125 Hz, $CDCl_3$) δ 172.0, 170.9, 151.0, 137.4, 136.5, 129.5, 125.5, 124.9, 120.1, 118.4, 117.8, 52.8, 52.5, 29.9, 23.1; IR (KBr) 3417, 1728, 1653, 1289, 1242 cm^{-1}. HRMS Calcd for $[M]^+$ $C_{15}H_{17}N_3O_4$: 303.1219. Found: 303.1215.

UV−Visible Spectra. Ground-state UV−visible spectra of tyrosine, 3-aminotyrosine, and compound **1** in 0.1 M sodium bicarbonate/0.06 M *tert*-butyl alcohol buffer, pH 10, were recorded at room temperature on a Hewlett-Packard (8452) diode-array spectrophotometer in a 0.2-cm path length quartz cuvette. Time-resolved absorbance difference spectra (post- minus pre-photolysis) of tyrosine and compound **1** were recorded at room temperature in the same deoxygenated buffer by an optical multichannel analyzer.[11] The spectra were collected in a 0.2 × 0.05 cm quartz cuvette at 5−8 delay times between 30 ns and 10 ms following excitation at 266 nm (Nd:YAG, 7 ns pulse, 300 μJ/mm^2). The spectral changes were probed along the 0.2-cm path length at 90° to the laser photolyzing beam. Prior to recording of the time-resolved spectra, the samples were saturated with nitrous oxide, which removes the spectral contribution of a solvated electron according to: $N_2O + e^-(aq) \rightarrow OH^\bullet + N_2 + OH^-$.[16] Because the hydroxyl radical may initiate unwanted reactions and thus interfere with the transient spectra, *tert*-butyl alcohol was added to quench the hydroxyl radical. The resulting β-hydroxyl radical produced from the alcohol is unlikely to interfere with the transient spectra.[16] Each difference spectrum represents an average of 16 and 20 individual spectra for the tyrosine and the cross-linked His−phenol complex, respectively. Baseline fluorescence was subtracted automatically. The time-resolved difference spectra were analyzed by singular value decomposition (SVD) and global exponential fitting with Matlab software (Mathworks), as previously described.[11,17,18]

(12) Chen, Y. R.; Sturgeon, B. E.; Gunther, M. R.; Mason, R. P. *J. Biol. Chem.* **1999**, *274*, 3308−3314.
(13) MacMillan, F.; Kannt, A.; Behr, J.; Prisner, T.; Michel, H. *Biochemistry* **1999**, *38*, 9179−9184.
(14) Proshlyakov, D. A.; Pressler, M. A.; DeMaso, C.; Leykam, J. F.; DeWitt, D. L.; Babcock, G. T. *Science* **2000**, *290*, 1588−1591.
(15) McCauley, K. M.; Vrtis, J.; Dupont, J.; Van der Donk, W. A. *J. Am. Chem. Soc.* **2000**, *122*, 2403−2404.
(16) Bent, D. V.; Hayon, E. *J. Am. Chem. Soc.* **1975**, *97*, 2599−2606.
(17) Sucheta, A.; Georgiadis, K. E.; Einarsdóttir, Ó. *Biochemistry* **1997**, *36*, 554−565.
(18) Van Eps, N.; Szundi, I.; Einarsdóttir, Ó. *Biochemistry* **2000**, *39*, 14576−14582.

The difference spectra of the intermediates were extracted on the basis of a unidirectional sequential scheme. The time-resolved spectra of compound **1** were also recorded in the presence of dioxygen in 10 mM borate−NaOH, pH 11.

Spectrophotometric Titrations. Spectrophotometric titrations of *p*-cresol (pH = 3.6−11.2), tyrosine (pH = 8.08−11.82), and compound **1** (pH = 2.5−10.63) were recorded on a diode-array spectrophotometer (HP 8452). The samples were prepared in aqueous solutions of 0.1 M potassium chloride, and the spectra were corrected for dilution by the base titrant.

The pK_a values of tyrosine, *p*-cresol, and compound **1** were determined from the experimental absorption spectra recorded over a wide pH range by SVD and global pK fitting. The SVD significantly reduces the number of parameters required for the global fitting.[19] Below is a brief description of the technique used to analyze the titration of compounds with multiple dissociation steps.

The absorption data matrix of a mixture of k components can be written as a product of two matrixes:

$$\mathbf{A}(\lambda, \mathrm{pH}) = \mathbf{E}(\lambda)\mathbf{C}(\mathrm{pH})$$

where $\mathbf{E}(\lambda)$ is an $m \times k$ matrix whose columns are the extinction coefficients of the components measured at m wavelength (λ) values, and $\mathbf{C}$(pH) is a $k \times n$ matrix whose rows are the concentrations of the components at n pH values. For simplicity, the arguments will be omitted from subsequent formulas. The term component used in the analysis does not necessarily imply that a single chemical entity is present. The spectrum of a given component may represent the superposition of spectra from two or more related structures, such as a neutral and a zwitterionic structure having the same protonation state.

In the SVD analysis, three data matrixes, **U**, **S**, and **V**, are generated such that $\mathbf{A} = \mathbf{USV}'$ where **U** is an $m \times n$ matrix and $\mathbf{V}'$, the transpose of **V**, is an $n \times n$ matrix. The columns of **U** are the orthogonal spectra and the columns of **V** contain the pH dependence of these spectra. The column vectors in the **U** and **V** matrixes are arranged in the order of their significance, which is reflected by the corresponding singular values in the **S** diagonal matrix. Only a limited number of the most significant **U** and **V** vectors are needed to reproduce the data matrix within the experimental noise. The scaled, significant orthogonal vectors can be represented by the product of the **U** and **S** matrixes, **US**.

The spectra of the components, **E**, which are usually not orthogonal, can be represented by a linear combination, represented by a matrix **L**, of the significant, scaled orthogonal vectors: $\mathbf{E} = \mathbf{USL}$. Accordingly, the data matrix can be written as $\mathbf{A} = \mathbf{USLC}$, where the pH dependence is given by $\mathbf{V}' = \mathbf{LC}$. As shown below, the entries in **C** are calculated by use of a function that describes the dissociation process, and the pK_a values are obtained from the best fit to this function. The calculations become greatly simplified compared to fitting the data matrix directly, because only a limited number of the significant **V** vectors are involved in the fitting.

The function describing the concentration pH dependence of the components reflects the chemical nature of the compounds under study. For a mixture of independent acids and bases with a single dissociation step, the simple Henderson−Hasselbalch formula is used.[19] For compounds with multiple dissociation steps, the formula is more complicated. The derivation below applies to the so-called macroscopic dissociation constants, which reflect the overall protonation changes in the system. We assume that an acid has k forms with different pK_a values. The proton dissociation of the ith state is described by the dissociation constant, K_i:

$$K_i = (A_{i+1}H)/A_i$$

where H and A denote the concentrations of the protons and acid in its different dissociation forms, respectively. The total acid concentration, A_0, is the sum of the concentrations of all the components with different pK_a values present in the system:

$$A_0 = A_1 + A_2 + A_3 + ... + A_{k-1} + A_k$$

Since each concentration can be calculated from the previous one

$$A_0 = A_1 + (K_1/H)A_1 + (K_1K_2/H^2)A_1 + ... + (K_1K_2...K_{k-2}K_{k-1}/H^{k-1})A_1$$

or in a more compact form

$$A_0 = (1 + \sum_{i=1}^{k-1} P_i/H^i)A_1$$

where

$$P_i = \prod_{j=1}^{i} K_j$$

The expressions for the concentrations of the individual components are as follows:

$$A_1 = A_0/(1 + \sum_{i=1}^{k-1} P_i/H^i)$$

$$A_2 = A_0/(P_1/H)/(1 + \sum_{i=1}^{k-1} P_i/H^i)$$

and finally

$$A_k = A_0(P_{k-1}/H^{k-1})/(1 + \sum_{i=1}^{k-1} P_i/H^i)$$

In practice, we use pK and pH as variables, and P_i/H^i is replaced by the power function of 10, where the power is (ipH − $\Sigma_{j=1}^{i}$pK_j).

Each row of the **C** matrix contains the concentrations of the corresponding component calculated at n pH values. If two or more compounds are present with multiple dissociation steps, then the concentration matrix is repeated for each compound. For compounds with a single dissociation step, these formulas reduce to the Henderson−Hasselbalch equation. The best least-squares fit of the **LC** matrix to the $\mathbf{V}'$ matrix provides a set of pK_a values and an **L** matrix, which is used to calculate the spectra of the components, $\mathbf{E} = \mathbf{USL}$, as already discussed.

EPR Spectroscopy. EPR spectra were acquired on a Bruker (Billerica, MA) EMX spectrometer equipped with a TE cavity and a Wilmad (Buena, NJ) temperature control dewar. The sample temperature was maintained at 77 K. UV photolysis flashes at 266 nm were supplied by a frequency-quadrupled pulsed YAG laser (Continuum, Santa Clara, CA). The sample was illuminated with 5 (for tyrosine, ^{13}C(6) tyrosine, and H-His-Tyr-OH dipeptide) or 10 (compound **1**) flashes in the cavity at a frequency of 10 Hz; the energy of the laser pulses was 35−37 mJ. Samples were 100 mM and contained 10 mM borate−NaOH, pH 11. To mimic the conditions for the FT-IR data acquisition, samples were concentrated in the EPR tube with a stream of cold nitrogen before data acquisition. Spectral conditions were as follows: frequency, 9.21 GHz; microwave power, 0.2 mW; modulation, 100 kHz; modulation amplitude, 2 G; time constant, 1.3 s; data acquisition time, 168 s; number of scans, 4. Spectra were obtained from two different samples. EPR spectra were simulated with a program previously described.[20] Spin quantitation was performed by double integration through the use of Igor Pro software (Lake Oswego, OR).

(19) Shrager, R. I.; Hendler, R. W. *Anal. Chem.* **1982**, *54*, 1147−1152.

(20) Hoganson, C. W.; Babcock, G. T. *Biochemistry* **1992**, *31*, 11874−11880.

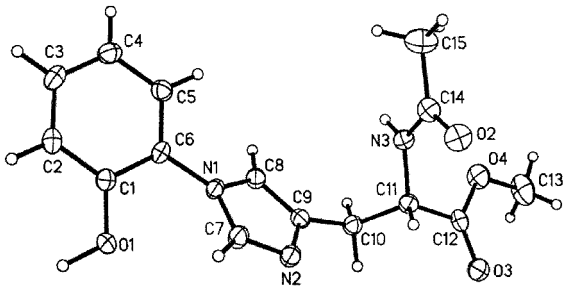

Figure 1. X-ray crystal structure of the cross-linked model histidine−phenol compound, 1-*o*-phenol(acetyl)histidine methyl ester (compound **1**).

FT-IR Spectroscopy. FT-IR ground-state spectra and difference FT-IR spectra associated with the photolysis reaction were obtained through the use of a Nicolet (Madison, WI) 60SXR spectrometer, equipped with a liquid nitrogen-cooled MCT-B detector and a Hansen (Santa Barbara, CA) cryostat. The experimental conditions were the same as those described for the EPR measurements. The sample holder was equipped with two CaF_2 windows. Samples were concentrated on a window with a stream of cold nitrogen before data acquisition. Difference spectra were constructed from data obtained before and after photolysis. Ground-state spectra were obtained before photolysis. Spectral conditions were as follows: resolution, 4 cm^{-1}; apodization function, Happ−Genzel; zero-filling, 1 level; data acquisition time, 1 min. Before the beginning of FT-IR data acquisition, the FT-IR sample was mounted in a Hitachi (Danbury, CT) 3000 UV−vis spectrophotometer and the absorption spectrum was measured. The absorption at 294 nm was used to correct the FT-IR spectrum for concentration and path length. Alternatively, the FT-IR spectrum was corrected for the amplitude of the C−C stretching vibration (1500 cm^{-1}) or the C−O stretching vibration (∼1260 cm^{-1}) in the ground-state absorption spectrum. Similar results were obtained with all three correction methods. Difference spectra were obtained from 2−8 different samples and averaged.

Results

Structure of the His−Phenol Complex. Complete spectroscopic data (IR, ^1H and ^{13}C NMR, and mass spectrometry) were obtained in order to verify the structure of the His−phenol compound. The structure was confirmed by single-crystal X-ray analysis, the results of which are shown in Figure 1. The dihedral angle (−36.3°) between the phenol and imidazole functionalities in this structure is similar in magnitude to that observed in the native enzyme (44°).[3]

Ground-State Absorption Spectra. Figure 2 shows the ground-state UV−visible spectra of tyrosine, the histidine−tyrosine dipeptide, 3-aminotyrosine, and compound **1** in 0.1 M $NaHCO_3$/0.06 M *tert*-butyl alcohol buffer, pH 10. Because pH 10 is below the pK_a of tyrosine (10.1), there are two maxima at 280 and 298 nm, corresponding to the protonated and deprotonated forms of tyrosine, respectively. The same maxima are observed for the histidine−tyrosine dipeptide. On the other hand, a single maximum is observed in the spectra of both compounds with amine substitution ortho to the phenolic hydroxyl group, 3-aminotyrosine and compound **1**, indicating that both are in the fully deprotonated anionic form at pH 10.

Spectrophotometric Titrations. To verify that the pK_a of the phenolic proton on tyrosine is lowered as a result of the cross-link, spectrophotometric titrations were carried out on *p*-cresol (pH = 3.6−11.2) (Figure 3A), tyrosine (pH = 8.08−11.82; not shown), and compound **1** (pH = 2.5−10.63) (Figure 4A). SVD and global pK fitting provided the spectra of the

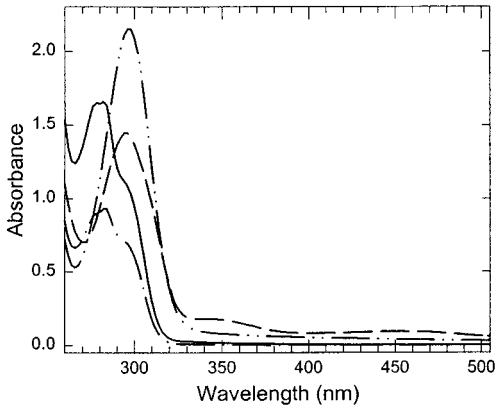

Figure 2. UV−visible spectra of tyrosine (3.24 mM) (−·−), the histidine−tyrosine dipeptide (6.65 mM) (—), 3-aminotyrosine (1.79 mM) (− − −), and compound **1** (1.78 mM) (−··−). The buffer was 0.1 M $NaHCO_3$/0.06 M *tert*-butyl alcohol, pH 10.

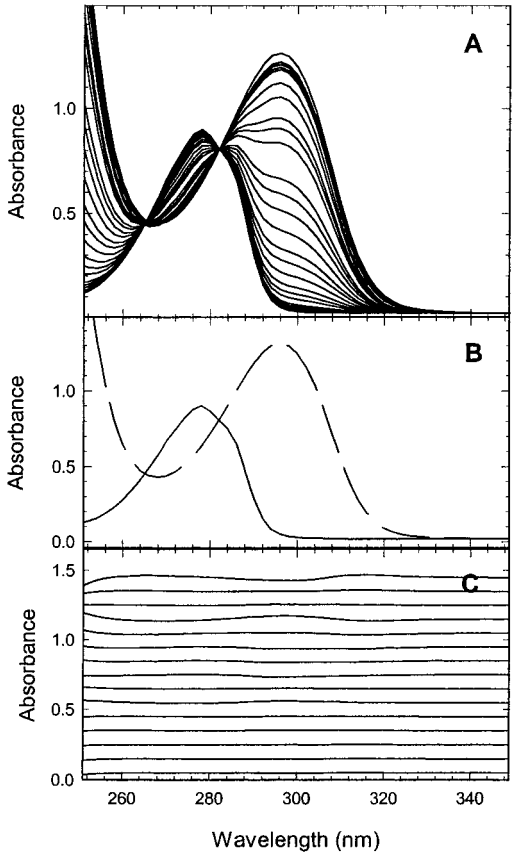

Figure 3. (Panel A) Spectrophotometric titration of an aqueous solution of *p*-cresol (0.5 mM) from pH 3.6 to 11.2. The data were analyzed by SVD and global pK_a fitting, which provided the spectral forms of the different protonation states of the compound (panel B: solid line, protonated; dashed line, deprotonated). The residuals show the difference between the fit and the data for a single pK_a of 10.05 (panel C).

intermediate forms and their pK_a values. For *p*-cresol, a single pK_a of 10.05 was obtained, while two pK_a values, 8.65 and 10.10, were observed for tyrosine. The two pK_a values are attributed to the terminal amine and the phenolic side chain, respectively, and are in good agreement with previously reported values,[15,16,21] thus validating our analysis method. Analysis of the titration spectra of compound

(21) *CRC Handbook of Chemistry and Physics*, 58th ed.; CRC Press: Boca Raton, FL, 1978.

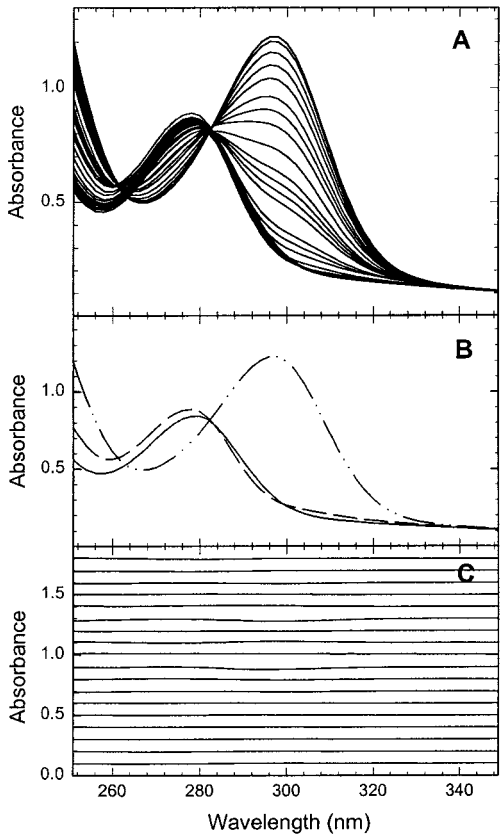

Figure 4. (Panel A) Spectrophotometric titration of an aqueous solution of the His−phenol cross-linked compound (compound **1**) (1.0 mM) from pH 2.5 to 10.63. The data were analyzed by SVD and global pK_a fitting, which provided the spectral forms of the different protonation states of compound **1** (panel B: —, fully protonated; − − −, imidazole deprotonated; −··−, fully deprotonated). The residuals show the difference between the fit and the data for pK_a values of 5.54 and 8.34 (panel C).

1 resulted in two pK_a values of 5.54 and 8.34, which are assigned to the imidazole group and phenol, respectively. The two pK_a values represent a unique fit and converged on the same values regardless of the initial starting values. Figures 3B and 4B show the spectra of the different protonation states of the *p*-cresol and compound **1**, respectively. The accuracy of the fit is reflected in the residuals (Figures 3C and 4C), which represent the difference between the reproduced data and experimental data.

Time-Resolved UV−Vis Difference Spectra. The radical forms of tyrosine and compound **1** were generated in vitro by UV photolysis. UV photolysis should generate a tyrosyl radical in compound **1**, because the oxidation potential is expected to be only 66 mV more positive, when compared to tyrosine.[15] Figure 5, panels A and C, show the UV−visible (350−675 nm) time-resolved difference spectra (post- minus pre-photolysis) of tyrosine and compound **1,** respectively, in a deoxygenated buffer solution following excitation at 266 nm at room temperature. The tyrosine time-resolved difference spectra were recorded at five delay times: 1 μs, 10 μs, 30 μs, 100 μs, and 1 ms. The difference spectra, with a maximum at ∼400 nm (Figure 5A), are consistent with the formation of a tyrosyl radical.[16,22,23] The time-resolved difference spectra of compound **1** (Figure 5C) were recorded at eight delay times: 30 ns, 100 ns, 400 ns, 1 μs, 10 μs, 100 μs, 1 ms, and 10 ms. The difference spectra show a unique absorption band at ∼500 nm. Another peak was observed at ∼330 nm. The peak at 500 nm clearly decays more rapidly than the 330 nm band, indicating that at least two species contribute to the spectra. The same spectra were observed in the presence of dioxygen (not shown).

The time-resolved difference spectra of the tyrosine (Figure 5A) were satisfactorily fitted with a single exponential (77 μs) by SVD and global exponential fitting. The spectrum of the intermediate is shown in Figure 5B and is consistent with the formation of a tyrosyl radical.[16,22,23] Time-resolved difference spectra of the histidine−tyrosine dipeptide also revealed a single peak at ∼400 nm (not shown).

To fit the transient data of compound **1**, two exponentials with apparent lifetimes of 1.4 and 9.8 μs were required, supporting the presence of two species, the spectra of which are shown in Figure 5D. The first species, with a lifetime of ∼1 μs, was found to have absorption maxima at ∼325 and ∼500 nm. The second species, which decayed with a lifetime of ∼10 μs, displayed a peak at ∼330 nm and a shoulder at ∼380 nm.

EPR Spectra. EPR spectroscopy and UV photolysis at 77 K have been shown to generate Tyr• radicals in basic aqueous solutions.[24] In Figure 6, the EPR spectra of the radicals produced by photolysis in solutions of tyrosine (A), ^{13}C(6) tyrosine (B), the His-Tyr dipeptide (C), and compound **1** (D) are shown as solid lines. The EPR line shape of the radical produced in frozen tyrosinate solutions (Figure 6A) was similar to results previously obtained.[24−26] As expected, there was no detectable signal produced from the borate buffer alone (Figure 6A, dotted line). Spectral broadening upon ^{13}C labeling of the ring (Figure 6B) was consistent with the assigned distribution of unpaired spin density.[24,25] While the EPR line shape derived from the His-Tyr dipeptide (Figure 6C) resembled spectra derived from tyrosinate (Figure 6A, solid line), a significant line shape perturbation was observed in compound **1** (Figure 6D, solid line).

The *g* values of the radicals were 2.0050 ± 0.0001 for tyrosine, 2.0054 ± 0.0001 for ^{13}C(6) tyrosine, 2.0046 ± 0.0001 for the His-Tyr dipeptide, and 2.0052 ± 0.0001 for compound **1**. Given the standard deviation, the *g* values of radicals produced in tyrosine and in compound **1** are indistinguishable. Quantitation of the amount of signal produced in tyrosine and in compound **1** gave results that were also indistinguishable, given the standard deviation (∼±10%). These results suggest that each radical is deprotonated and that there is little change in spin density on the phenolic oxygen when tyrosine and compound **1** are compared.[27]

To test this idea, the EPR signals arising from tyrosine (Figure 6A, solid line) and compound **1** (Figure 6D, solid line) were simulated, and the simulations are shown superimposed in Figure 6A,D as dashed lines. The parameters (Table 1) used for the tyrosyl radical simulation (Figure 6A, dashed line) were similar to those previously employed.[25] The EPR line shape derived from the cross-linked compound could be simulated (Figure 6D, dashed line) by removal of the couplings to the

(22) Land, E. J.; Porter, G. *Trans. Faraday Soc.* **1963**, *59*, 2016−2026.
(23) Tripathi, G. N. R.; Schuler, R. H. *J. Chem. Phys.* **1984**, *81*, 113−121.
(24) Barry, B.; El-Deep, M. K.; Sandusky, P. O.; Babcock, G. T. *J. Biol. Chem.* **1990**, *265*, 20139−20143.
(25) Hulsebosch, R. J.; Van der Brink, J. S.; Niewenhuis, A. M.; Gast, P.; Raap, J.; Lugtenburg, J.; Hoff, A. J. *J. Am. Chem. Soc.* **1997**, *119*, 8685−8694.
(26) Warncke, K.; Perry, M. S. *Biochim. Biophys. Acta* **2001**, *1545*, 1−5.
(27) Dixon, W. T.; Murphy, D. *J. Chem. Soc., Faraday. Trans. 2* **1976**, *72*, 1221−1229.

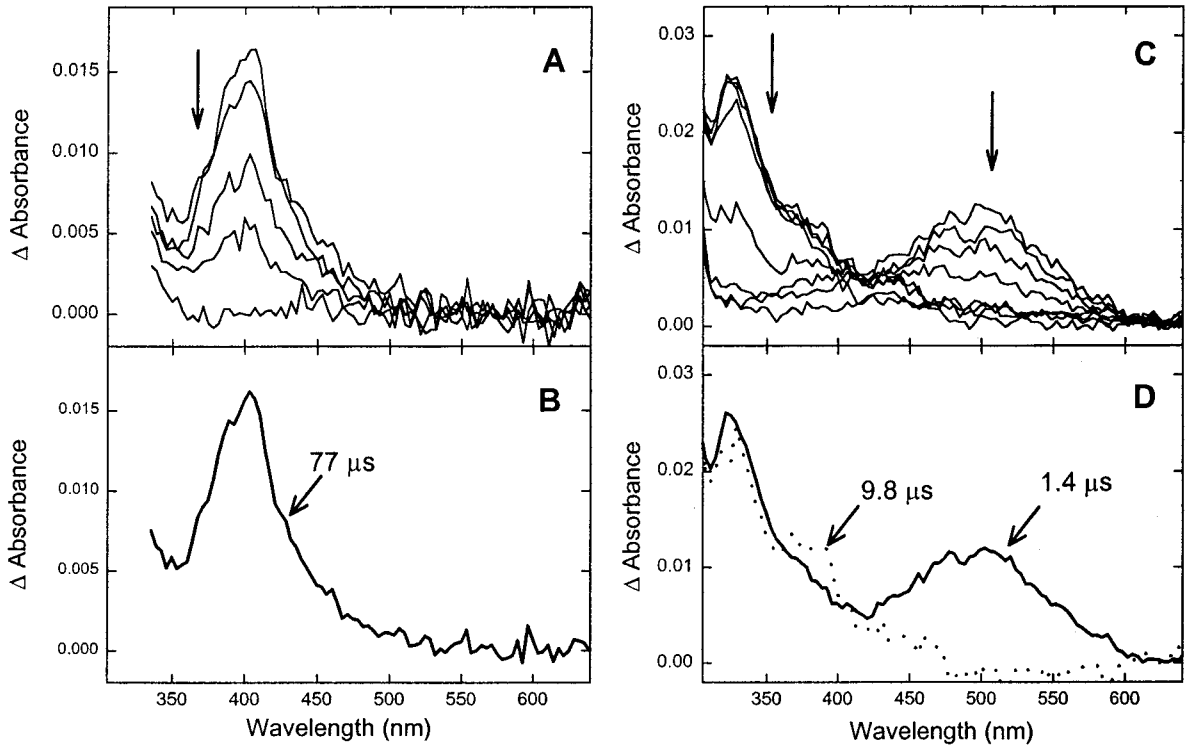

Figure 5. (A, C) Time-resolved difference spectra (post- minus pre-photolysis) of aqueous solutions of (A) tyrosine (3.24 mM) and (C) the His−phenol cross-linked compound (1.78 mM) following excitation at 266 nm (Nd:YAG, fourth harmonic 7 ns pulse) at room temperature. The laser power was 300 mJ/mm^2. The probe beam was a xenon flash lamp, and the signals were detected by an optical multichannel analyzer with a 100 μm slit and 200 ns gate. The buffer was 0.1 M $NaHCO_3$/0.06 M *tert*-butyl alcohol (pH 10), and the samples were purged with N_2O just prior to use (to remove absorption contribution from the solvated electron). (B, D) Intermediate spectra of tyrosine (B) and the His−phenol complex (D) resulting from the SVD/global exponential fitting and on the basis of a unidirectional sequential mechanism. A single apparent lifetime of 77 μs was obtained for tyrosine. The apparent lifetimes for compound **1** were 1.4 and 9.8 μs.

tyrosine β-protons and addition of a relatively isotropic, large hyperfine coupling to the hydrogen at ring position 4 (Table 1). An isotropic hyperfine tensor is not expected for an α-proton but was required to fit the EPR line shape with this parameter set. A small hyperfine coupling for the imidazole nitrogen was included, but the exact value between 0 and 1.5 G did not have a dramatic effect on the simulation result. A small nitrogen coupling is consistent with the unperturbed *g* value of this radical, compared to tyrosine, and with a relatively unperturbed phenoxyl spin density distribution. The results suggest that the EPR spectrum of the tyrosyl radical is comparatively insensitive to *o*-imidazole addition.

FT-IR Ground-State Spectra. Another optical property of compound **1** was compared to tyrosine. Figure 7 shows the ground-state FT-IR spectra of tyrosine (A), ^{13}C(6) tyrosine (B), the His-Tyr dipeptide (C), and compound **1** (D). Spectral contributions from the borate buffer blank were subtracted. Residual water contributions are presumably due to solvent interaction with the tyrosine-related compounds and were observed at ∼2000 (combination band, not shown) and ∼1650 cm^{-1} (Figure 7, O−H bend). When the compound contains a terminal amino group, a contribution from the N−H bending mode is also expected in the 1650 cm^{-1} region.[28]

(A) Tyrosinate C−O Stretching Vibration. Several tyrosinate vibrational modes are anticipated in the 1300−1100 cm^{-1} region,[29,30] including a C−O stretching mode ($\upsilon_{7a'}$), expected at ∼1260 cm^{-1}, and a C−C−H bending mode (υ_{9a}), expected at ∼1170 cm^{-1}.[29,30] In the tyrosinate spectrum (Figure 7A), a band was observed at 1266 cm^{-1}, which shifted upon ^{13}C labeling (Figure 7B). The frequency and the magnitude of the ^{13}C shift support the assignment of this band to $\upsilon_{7a'}$ of the tyrosinate species.[29,30] A spectral feature with similar frequency and intensity was observed in the His-Tyr dipeptide. In compound **1**, a band at 1265 cm^{-1} was much less intense, and a band at 1241 cm^{-1} was also observed (Figure 7D). The fact that two bands are observed may be attributed to a unique intermolecular hydrogen-bonding interaction in the ground state of compound **1**.[29,30]

The 1173−1172 cm^{-1} band in tyrosine (Figure 7A) and the His-Tyr dipeptide (Figure 7C) is assigned to υ_{9a}, a C−H bending mode.[29,30] As expected, this band was shifted in compound **1** (Figure 7D), where one of the *o*-hydrogens has been removed and replaced with an imidazole nitrogen.

(B) Tyrosinate Ring Stretching Vibrations. Bands at 1602−1601 and 1501−1500 cm^{-1} were observed in both tyrosine (Figure 7A) and the His-Tyr dipeptide (Figure 7C). These spectral features downshifted to 1562 ($\Delta = -40$ cm^{-1}) or 1549 ($\Delta = -53$ cm^{-1}) and 1464 ($\Delta = -36$ cm^{-1}) cm^{-1}, respectively, upon ^{13}C(6) tyrosine labeling (Figure 7B). The observed frequencies and isotope shifts support the assignment of these bands to ring stretching modes, υ_{8a} and υ_{19a}, of the tyrosinate species.[23,29−32] In compound **1**, bands at 1591 and 1509 cm^{-1}

(28) Bellamy, L. J. *The infrared spectra of complex molecules*; Chapman and Hall: London, 1980; Vol. I.
(29) Takeuchi, H.; Watanabe, N.; Satoh, Y.; Harada, I. *J. Raman Spectrosc.* **1989**, *20*, 233−237.
(30) Mukherjee, A.; McGlashen, M. L.; Spiro, T. G. *J. Phys. Chem.* **1995**, *99*, 4912−4917.
(31) Chipman, D. B.; Lie, R.; Zhou, X.; Pulay, P. *Chem. Phys. Lett.* **1997**, *272*, 155−161.

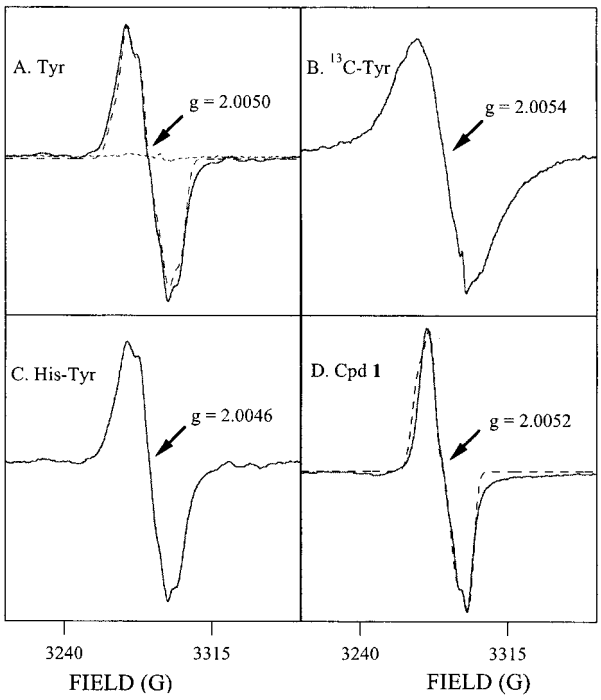

Figure 6. EPR spectra of free radicals produced in solutions of tyrosine (A, solid line), ^{13}C(6)-tyrosine (B), His-Tyr dipeptide (C), and His−phenol cross-linked compound (Cpd **1**) (D, solid line). Samples were 100 mM and also contained 10 mM borate−NaOH, pH 11. The radicals were generated by UV photolysis at 77 K; see Materials and Methods for conditions. EPR simulations are superimposed as the dashed lines in panels A and D. See Table 1 for parameters employed in the simulations. The dotted line in panel A is a negative control showing the results obtained with borate buffer alone.

Table 1. EPR Simulation Parameters[a]

hfi	A_{xx} (G)	A_{yy} (G)	A_{zz} (G)	A_{iso} (G)	ϕ
		Tyrosine[b]			
C2′-H	1.7	2.7	0.4	1.6	30
C3′-H	−9.6	−2.8	−7.0	−6.5	−23
C5′-H	−9.6	−2.8	−7.0	−6.5	23
C6′-H	1.7	2.7	0.4	1.6	−30
C1′-Hβ1	0.62	0.58	0.58	0.59	0
C1′-Hβ2	11.0	11.0	11.0	11.0	0
		Compound **1**[c]			
C2′-N	2.0	1.1	1.5	1.5	23
C3′-H	1.7	2.7	0.4	1.6	−30
C4′-H	−10	−10	−10	−10	0
C5′-H	1.7	2.7	0.4	1.6	30
C6′-H	−9.6	−2.8	−7.0	−6.5	−23

[a] EPR simulations were performed through the use of a computer program described in ref 20. Hyperfine interactions were obtained from ref 25 with minor modifications and are reported in Gauss. Euler angle ϕ represents the in-plane rotation of the hyperfine component about the g_z axis and is defined as positive clockwise rotation. Euler angles θ and ψ were set to 0 in each case. The isotropic g values were obtained experimentally. For numbering purposes, the hydroxyl group is at carbon number 4 for tyrosine, Tyr, and carbon number 1 for compound **1**. [b] Tyrosine: $g_{xx} = 2.0070$, $g_{yy} = 2.0046$, $g_{zz} = 2.0024$; line width = 2.7; frequency = 9.21 GHz. [c] Compound **1**: $g_{xx} = 2.0078$, $g_{yy} = 2.0054$, $g_{zz} = 2.0024$; line width = 2.0; frequency = 9.21 GHz.

may arise from υ_{8a} and υ_{19a} (Figure 7D). This preliminary assignment suggests that the effect of *o*-N substitution on ground-state phenolate vibrational modes is a downshift of the highest energy ring mode and an upshift of the υ_{19a} C−C/C−H vibration.

Two additional ring and C−C/C−H vibrational modes are expected in phenolate-containing compounds, υ_{8b} and υ_{19b}.[29,30] A 1560 cm^{-1} band was observed in the tyrosinate spectrum (Figure 7A), which may exhibit a ^{13}C(6) isotope shift of 11 cm^{-1} (Figure 7B). This spectral feature may correspond to υ_{8b}. Note that the asymmetric stretching vibration of the free carboxylate group is also expected to contribute to the spectrum at approximately 1560 cm^{-1}.[28] Spectra of tyrosine-containing dipeptides (data not shown) consistently exhibited a band at approximately 1580 cm^{-1} (Figure 7C) but did not show the 1560 cm^{-1} line. Therefore, the 1580 cm^{-1} band is a possible candidate for the υ_{8b} vibrational mode, which may have a shifted frequency in dipeptides. Accordingly, the spectral component at 1584 cm^{-1} can be attributed to υ_{8b} in compound **1** (Figure 7D). Assignment of υ_{19b} awaits a detailed normal coordinate analysis, but possible candidates are between 1440 and 1350 cm^{-1}; bands in this region exhibited small ^{13}C isotope shifts (Figure 7).

(C) Amide Bands. FT-IR spectra derived from both the His-Tyr dipeptide and compound **1** should exhibit amide I and II vibrational bands.[33] The spectral component at 1631 cm^{-1} in Figure 7C and at 1619 cm^{-1} in Figure 7D may be attributable to amide I in the dipeptide and the cross-link, respectively. The 1537 cm^{-1} band in Figure 7C is a candidate for the amide II vibrational mode in the His-Tyr dipeptide. The location of the amide II band in compound **1** is not obvious, but this band may overlap the putative tyrosinate ring mode at ∼1580 cm^{-1} (Figure 7D).

(D) Other Vibrational Modes. Bands at 1437, 1419, 1360, and 1331 cm^{-1} in tyrosine (Figure 7A) may originate from υ_{19b}, C−C/C−H bending modes of the tyrosinate α and β carbon atoms, or from the carboxylate symmetric stretching vibration. This spectral region was altered in the His-Tyr dipeptide (Figure 7C) and in compound **1** (Figure 7D). Remaining unique bands in the spectrum of compound **1** (Figure 7D) at 1478, 1451, and 1308 cm^{-1} are potentially attributable to vibrations of the *o*-substituted imidazole moiety (see below), to C−CH_3 bending modes, and to coupled vibrations arising from both the imidazole and the phenolate moieties. The ester C═O of compound **1** should also make a spectral contribution between 1750 and 1720 cm^{-1}; this contribution may be obscured by the broad band at approximately 1660 cm^{-1}.[28]

FT-IR Spectra Associated with Photolysis. UV photolysis was performed to examine the vibrational spectrum of the tyrosyl radical. Vibrational spectroscopy has previously shown that oxidation of phenolate and tyrosinate upshifts the C−O stretching vibration and perturbs aromatic ring stretching vibrations.[23,29,30,34,35] Our EPR control experiments verify that the neutral tyrosyl radical can be generated in tyrosinate solutions under these conditions (see discussion above). Figure 8B shows the FT-IR difference spectrum associated with the oxidation of tyrosinate at 77 K. Positive features in these data arise from unique vibrational modes of the neutral Tyr$^{\bullet}$ radical, while negative features arise from unique modes of the tyrosinate ground state. As expected, photolysis experiments performed on the borate buffer alone gave a flat baseline (Figure 8A). Photolysis-induced difference spectra were also acquired from ^{13}C(6)-tyrosine (Figure 8C), the His-Tyr dipeptide (Figure 8D), and compound **1** (Figure 8E). Each spectrum (Figure 8B−E)

(32) Nwobi, O.; Higgins, J.; Xuefeng, Z.; Ruifeng, L. *Chem. Phys. Lett.* **1997**, *272*, 155−61.
(33) Krimm, S.; Bandekar, J. *Adv. Protein Chem.* **1986**, *38*, 181−364.
(34) Qin, Y.; Wheeler, R. A. *J. Chem. Phys.* **1995**, *102*, 1689−1698.
(35) Kim, S.; Barry, B. A. *J. Phys. Chem. B* **2001**, *105*, 4072−4083.

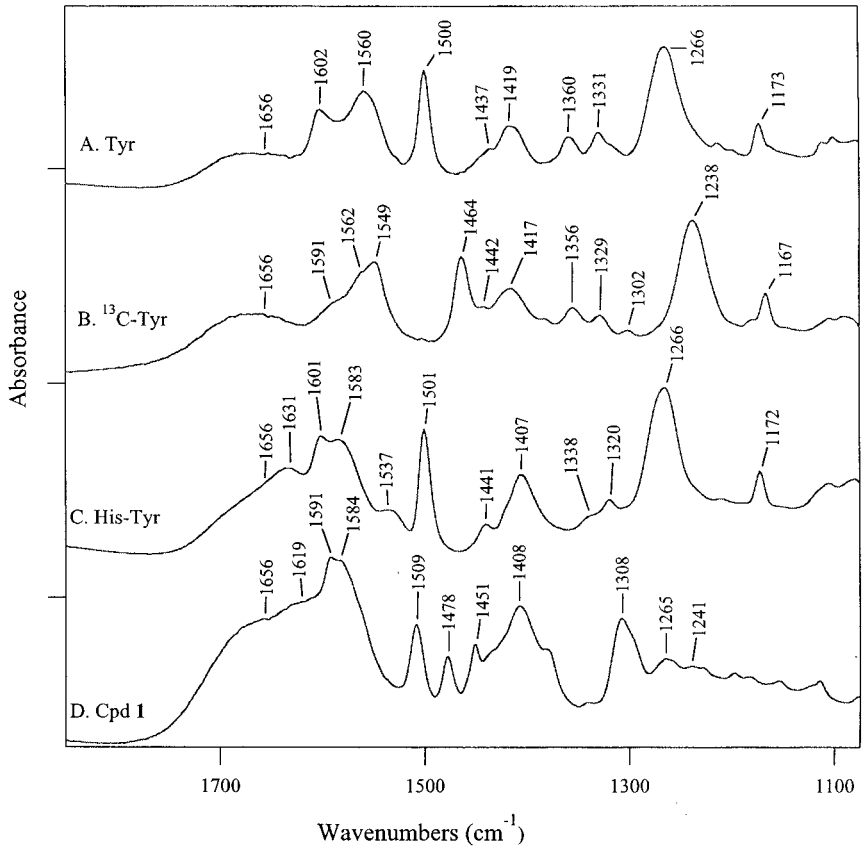

Figure 7. FT-IR spectra of tyrosine (A), ^{13}C(6)-tyrosine (B), His-Tyr dipeptide (C), and His−phenol cross-linked compound (compound **1**) (D). Samples were 100 mM and also contained 10 mM borate−NaOH, pH 11. See Materials and Methods for conditions. The borate contributions have been subtracted from these data. The tick marks on the *y*-axis correspond to 0.4 absorbance unit.

exhibited a broad positive band between 1665 and 1650 cm^{-1}, which we assign to perturbations of OH (water) and NH (amine) bending modes upon tyrosinate oxidation. The NH perturbation will be described in detail in a future publication.

(A) Negative Spectral Contributions. Perturbed tyrosinate vibrations should be observed in the difference spectrum as negative bands (see section above). In Figure 8B, negative lines at 1606, 1500, 1263, and 1173 cm^{-1} were observed in the tyrosine photolysis spectrum. Corresponding bands (frequencies within 5 cm^{-1}) were found in the ground-state tyrosinate spectrum (Figure 7A) and were assigned to C−C ring stretching, C−C/C−H stretching, C−O stretching, and C−H bending modes, respectively. These negative bands in Figure 8B were downshifted to 1560 or 1547, 1466, 1235, and 1167 cm^{-1} in ^{13}C(6)-tyrosine (Figure 8C). They were observed at 1603, 1502, 1263, and 1173 cm^{-1} in the His-Tyr dipeptide (Figure 8D) and at 1592 (shoulder), 1511, and 1265 cm^{-1} in compound **1** (Figure 8E). A negative band between 1570 and 1530 cm^{-1} in tyrosine (Figure 8B) and 1577−1574 cm^{-1} in the dipeptide (Figure 8D) and compound **1** (Figure 8E) may be assignable to υ_{8b}. This band may have a frequency of 1547 cm^{-1} in the ^{13}C isotopomer (Figure 8C). A band at 1415−1410 cm^{-1} in the dipeptide (Figure 8D) and in compound **1** (Figure 8E) may be assignable to υ_{19b}, although this assignment awaits further analysis (see discussion above).

Unique negative features in spectra derived from compound **1** may be assigned to C−C/C−N stretching and C−H bending vibrations of the *o*-substituted imidazole ring.[36] Alternatively, these may correspond to coupled vibrational modes, as discussed above. Likely candidates had frequencies of 1479, 1451, and 1303 cm^{-1} (Figure 8D). These spectral features were unique to the His−phenol cross-link and had similar frequencies in the ground-state spectrum (Figure 7D). Observation of these bands in the difference spectrum suggests that the photolysis reaction perturbs force constants in the imidazole group of compound **1**.

(B) Positive Spectral Contributions. The tyrosyl radical is expected to contribute positive lines in Figure 8. Candidates for tyrosyl ring stretching modes were observed at 1620 and 1577 cm^{-1} (Figure 8B). These bands shifted either to 1611 or to 1527−1505 cm^{-1}, respectively, upon ^{13}C ring labeling (Figure 8C). On the basis of a previous Raman study of phenoxyl radical and ab initio calculations for phenoxyl and tyrosyl radicals, a frequency of ∼1620−1560 cm^{-1} and an isotope shift of ∼50−60 cm^{-1} are expected for υ_{8a}.[29−32,37] We tentatively assign the 1577 cm^{-1} band, which may exhibit a large ^{13}C isotope shift, to the υ_{8a} ring stretching vibration and the 1620 cm^{-1} band to another ring stretching vibration, possibly υ_{8b}. In the His-Tyr dipeptide and compound **1** (Figure 8D,E), the 1620 and 1577 cm^{-1} bands were not evident, perhaps because of cancellation in the difference spectrum.

The C−O stretch of the neutral phenoxyl radical has been previously assigned to a band at approximately 1505 cm^{-1}, while the C−O stretch of a tyrosyl radical has been assigned to a

(36) Majoube, M.; Vergoten, G. *J. Mol. Struct.* **1992**, *266*, 345−352.
(37) Qin, Y.; Wheeler, R. A. *J. Am. Chem. Soc.* **1995**, *117*, 6083−6092.

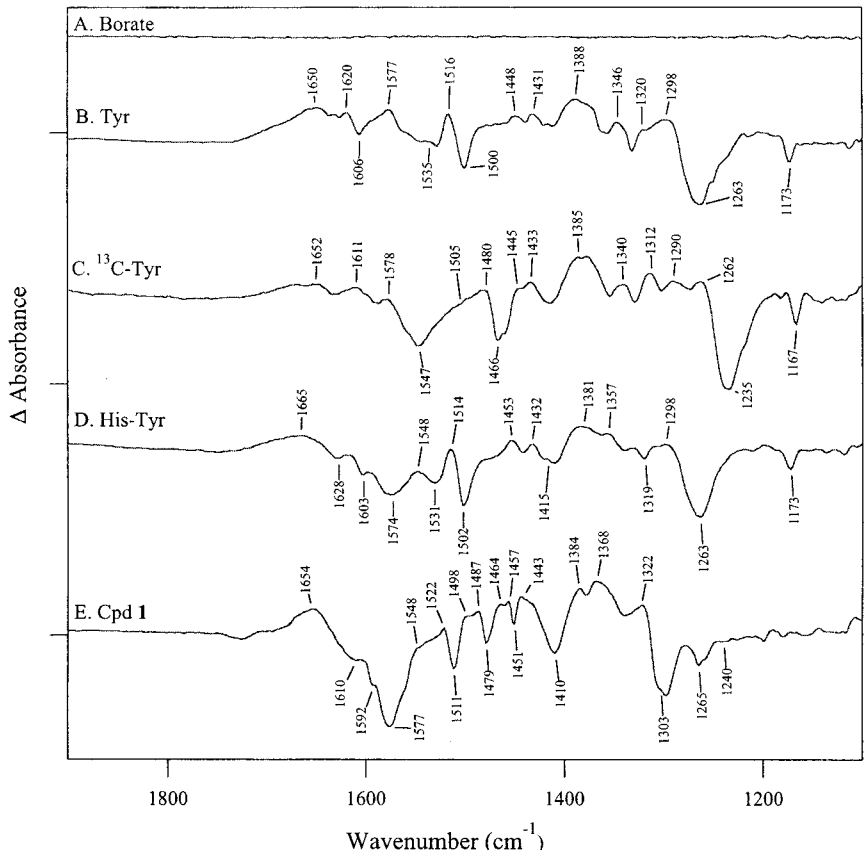

Figure 8. Difference FT-IR spectra associated with the production of radicals by UV photolysis at 77 K. The samples were borate alone (A), tyrosine (B), ^{13}C(6)-tyrosine (C), His-Tyr dipeptide (D), and His−phenol cross-linked compound (**1**) (E). The conditions are described in the Materials and Methods section and are identical to those employed for Figure 7. Individual difference spectra correspond to a total of 4 min of data acquisition, 2 min before UV photolysis and 2 min after photolysis. The difference spectra were constructed by directly ratioing data obtained after 5 (A−D) or 10 (E) laser flashes to data obtained before photolysis. To obtain the final signal-to-noise, spectra were averaged over two (A, C), eight (B), or three (D, E) different samples. Tick marks on the *y*-axis represent 2×10^{-2} absorbance unit.

band at 1515 cm^{-1}.[23,29,30,34,38,39] The tyrosyl radical produced in tyrosinate solutions exhibited a positive band at 1516 cm^{-1} (Figure 8B); this band apparently shifted to 1480 cm^{-1} upon ^{13}C labeling (Figure 8C). The frequency and magnitude of the isotope shift support the assignment of this band or a component of the band to a C−O stretching vibration (υ_{7a}).[29,30]

The His-Tyr dipeptide photolysis spectrum (Figure 8D) exhibited a band at 1514 cm^{-1}, which may have the same origin as the 1516 cm^{-1} line in tyrosine. In the photolysis spectrum of compound **1**, there was no vibrational mode observed at 1516−1514 or 1505 cm^{-1} (Figure 8E). However, bands at 1522, 1498, and 1487 cm^{-1} were observed. Our EPR studies, described above, showed that the *g* values of the radicals produced in tyrosine and in compound **1** are indistinguishable. This result is consistent with a largely unperturbed spin density distribution, so the most likely candidates for the C−O vibration are either the 1522 or the 1498 cm^{-1} band. Such a modest (∼1%) shift of the C−O vibrational mode in compound **1** is qualitatively consistent with the small nitrogen hyperfine coupling employed in the EPR simulations. A shift of the C−O vibration to 1522 or 1498 cm^{-1} also accounts for the lack of a 2115 cm^{-1} C−O/C−C−C combination band[23] in the photolysis spectrum of the cross-link (data not shown). A band at 1489 cm^{-1} in the P intermediate of cytochrome *bo* from *Escherichia coli* was recently attributed to the C−O stretching mode of a tyrosyl radical.[40]

Other vibrational bands were not observed in all samples. For example, spectra derived from the His-Tyr dipeptide and the His−phenol cross-link show a positive band at 1548 cm^{-1}, which was not observed in tyrosine. This band was also observed in dipeptides with other sequences (data not shown). The origin of this band and other unique spectral features will be examined in other work. Positive spectral bands between 1450 and 1300 cm^{-1} are tentatively assigned to C−C/C−H bending modes; this region was compound-specific, as expected. Overall, the photolysis spectrum obtained from compound **1** had a much more complex pattern of positive lines than those from tyrosine or the dipeptide. A subset of the positive bands may arise from perturbation of the structure of the substituted imidazole ring[36] upon tyrosinate oxidation. These vibrations either may be localized on the imidazole or may arise from coupled vibrational motions of the imidazole and phenoxyl ring. Candidates were observed at 1522, 1498, 1487, 1464, 1457, 1443, and 1368 cm^{-1}. One explanation of the cross-link FT-IR results is that phenolate oxidation results in a small delocalization of spin density onto the imidazole nitrogen of the cross-linked compound (see EPR results above) and that this spin delocalization alters force constants in the imidazole moiety.

(38) Johnson, C. R.; Ludwig, M.; Asher, S. A. *J. Am. Chem. Soc.* **1986**, *108*, 905−912.
(39) Berthomieu, C.; Boullais, C.; Neumann, J. M.; Boussac, A. *Biochim. Biophys. Acta* **1998**, *1365*, 112−116.
(40) Uchida, T.; Mogi, T.; Kitagawa, T. *Biochemistry* **2000**, *39*, 6669−6678.

Discussion

Synthesis of Compound 1. We report the synthesis of a model for a post-translationally modified amino acid residue, which is found at the active site of cytochrome *c* oxidase. The preparation of compound **1** and related compounds needed for future studies requires a method of synthesis that is mild enough to maintain the protection scheme and the absolute stereochemistry of amino acid precursors. Recently, we described such a method in the copper-catalyzed coupling of substituted imidazoles with aryllead(IV) reagents.[41] The mild reaction conditions allow for the incorporation of amino acid residues without racemization or adventitious deprotection. Reaction of *N*-α-acetylhistidine methyl ester (**2**)[42,43] and aryllead reagent (**3**)[44] at room temperature in CH_2Cl_2 produced coupled product **4** in 35% yield. Compound **4** was the only isomer isolated from the reaction mixture. Removal of the allyl protection group provided **1** in near-quantitative yield. As opposed to the compounds prepared in the previous study, compound **1** is devoid of additional aromatic moieties in the protection groups that could complicate spectroscopic analysis.[45] Efforts to synthesize the cross-linked histidine−tyrosine complex are underway.

Spectrophotometric Titrations. To evaluate the properties of compound **1** we carried out spectrophotometric titrations. The titrations resulted in two pK_a values of 5.54 and 8.34, which were assigned to protons on the ϵ-nitrogen of the imidazole and phenolic hydroxide, respectively. The pK_a values are similar to those reported by McCauley et al.[15] for 2-imidazol-1-yl-4-methylphenyl (5.54 and 8.60, respectively) but are slightly different from the pK_a values recently reported for 1-(*o*-hydroxyphenyl)-imidazole (7.86 and 6.12 for the phenol and imidazole, respectively).[46] However, in all cases, the pK_a of the phenolic proton is significantly lower than for the unsubstituted tyrosine, which is consistent with the cross-linked histidine−tyrosine facilitating proton delivery to the binuclear site in cytochrome *c* oxidase.[7,10,15] Therefore, the change in the electronic structure resulting from the substitution appears to lower the pK_a of the phenolic hydroxyl group compared to unsubstituted tyrosine.

Origin of the Transient Optical Intermediates. The analysis of the time-resolved optical absorption difference spectra of compound **1** indicated that two species were present. Our primary focus will be on the first, which showed absorption maxima at ∼500 and ∼325 nm and an apparent lifetime of 1.4 μs. We can exclude the possibility that this species represents a triplet, since identical time-resolved difference spectra were observed in the presence and absence of dioxygen. This is consistent with previous reports that no transient spectrum due to the triplet state can be observed at high pH.[16] The 1.4 μs species does not show an absorption band at ∼400 nm characteristic of unperturbed phenoxyl radical.[16,23] However, *o*-substitution on phenol enables appreciable conjugative effects that significantly red-shift the 400 nm peak of unperturbed phenol. For example, the spectrum of *o*-phenylphenol has been shown to have maxima at 500 and 360 nm.[22] Therefore, we attribute the first intermediate to a phenoxyl radical species. The large spectral shift (∼100 nm) between intermediate 1 and the unperturbed tyrosyl radical may also suggest significant mixing of the imidazole and phenoxyl electronic states in compound **1**.[22,23]

The nature of the second species (∼10 μs lifetime) is unknown, but we can exclude the formation of an oxidized histidine radical because its spectrum is inconsistent[47,48] with the spectrum we observe. Moreover, electron transfer from histidine to tyrosine would appear unlikely on the basis of their reported redox potentials.[49,50] The spectrum of the second species is quite similar to that of oxidized *N*-methylimidazole (pH 10) reported previously,[51] suggesting that the second species might be a secondary oxidation product.

EPR Results. The EPR spectrum, derived by photolysis of compound **1**, clearly establishes the generation of a paramagnetic species in this sample. Our EPR analysis of the paramagnetic species produced in compound **1** gives an isotropic *g* value of 2.0052. This *g* value is not significantly altered relative to the tyrosyl radical. However, it is distinct from the *g* values of an *o*-aminophenol radical, a histidine-OH radical, and a tryptophan radical, which are in the 2.0026−2.0037 range.[27,52,53] In addition, the value of the isotropic hyperfine coupling to nitrogen (∼1.5 G) is much smaller than the nitrogen coupling obtained in *o*-aminophenol (∼5−7 G).[54,55] These results suggest that while nitrogen substitution in *o*-aminophenol withdraws a significant amount of spin density from the phenoxyl ring, in compound **1** there is a modest perturbation of the spin density distribution. This is supported by recent calculations by Himo et al.,[56] which showed that the cross-link will have minor effects on the hyperfine coupling constants and spin distribution of the tyrosyl radical.

The EPR spectrum of the radical of compound **1** in Figure 6C differs from that published by McCauley et al.[15] of the radical form of 2-imidazol-1-yl-4-methylphenol. The difference is attributed to the 4-methyl group in the latter, which gives rise to three isotropic methyl protons (1:3:3:1 pattern) with A_{iso} of 10−11 G.[15] The EPR spectrum of compound **1** is also significantly different from the radical-generated *Paracoccus denitrificans* cytochrome oxidase EPR spectrum reported by MacMillan et al.[13] This signal was attributed to the cross-linked tyrosine radical. The putative cross-linked tyrosyl radical in cytochrome *c* oxidase exhibited large, nearly isotropic β-methylene proton couplings.[13] These protons are absent in compound **1** employed here.

FT-IR Results. Vibrational spectroscopy was also used to probe the structure of compound **1**. The ground-state FT-IR spectrum of the cross-link was significantly altered relative to

(41) Elliott, G. I.; Konopelski, J. P. *Org. Lett.* **2000**, *2*, 3055−3057.
(42) Mathews, H. R.; Rapoport, J. *J. Am. Chem. Soc.* **1973**, *95*, 2297−2303.
(43) Kasafírek, E.; Bartík, M. *Collect. Czech. Chem. Commun.* **1980**, *45*, 442−451.
(44) Morgan, J.; Pinhey, J. T. *J. Chem. Soc., Perkin Trans. 1* **1993**, 1673−1676.
(45) Elliott, G. I.; Konopelski, J. P. *Tetrahedron* **2001**, *57*, 5683−5705.
(46) Collman, J. P.; Wang, Z.; Zhong, M.; Zeng, L. *J. Chem. Soc., Perkin Trans. 1* **2000**, 1217−1221.
(47) Adams, G. E.; Aldrich, J. E.; Bisby, R. H.; Cundall, R. B.; Redpath, J. L.; Wilson, R. L. *Radiat. Res.* **1972**, *49*, 278−289.
(48) Parsons, B. J.; Al-Hakim, M.; Phillips, G. O. *J. Chem. Soc., Faraday Trans. 1* **1986**, 1575−1588.
(49) Brabec, V.; Mornstein, V. *Biophys. Chem.* **1980**, *12*, 159−165.
(50) Harriman, A. *J. Phys. Chem.* **1987**, *91*, 6102−6104.
(51) Rao, P. S.; Simic, M.; Hayon, E. *J. Phys. Chem.* **1975**, *79*, 1260−1263.
(52) Lassmann, G.; Eriksson, L. A.; Lendzian, F.; Lubitz, W. *J. Phys. Chem.* **2000**, *104*, 9144−9152.
(53) Lendzian, F.; Sahlin, M.; MacMillan, F.; Bittl, R.; Fiee, R.; Pötsch, S.; Sjöberg, B.-M.; Gräslund, A.; Lubitz, W.; Lassman, G. *J. Am. Chem. Soc.* **1996**, *118*, 8111−8120.
(54) Dixon, W. T.; Moghimi, M.; Murphy, D. *J. Chem. Soc., Faraday Trans. 2* **1974**, *70*, 1713−1720.
(55) Neta, P.; Fessenden, R. W. *J. Phys. Chem.* **1974**, *78*, 523−529.
(56) Himo, F.; Eriksoon, l. A.; Blomberg, M. A. A.; Siegbahn, P. E. M. *Int. J. Quantum Chem.* **2000**, *76*, 714−723.

tyrosine or to a histidine−tyrosine dipeptide and showed frequency shifts of bands assigned to ring C−C and C−O stretching vibrations, as well as other spectral changes. The frequency shifts of phenolate vibrational modes may be caused by a mass effect or by changes in intermolecular hydrogen bonding. New vibrational bands in the 1490−1290 cm^{-1} region, when the spectrum of compound **1** is compared to the His-Tyr dipeptide or tyrosinate spectrum, may arise from unique structural elements of the cross-linked compound as well as coupled vibrational motions of the phenolate and imidazole rings.

The difference FT-IR spectrum associated with the oxidation of compound **1** was also obtained and was found to be altered compared to the tyrosyl radical or to the tyrosyl radical produced in the dipeptide. New vibrational bands had frequencies consistent with a direct contribution of imidazole to the photolysis spectrum. *S*hifts of C−C and C−O bands assigned to the phenoxyl ring were also observed. These shifts may be associated with the small delocalization of spin density onto the imidazole moiety, which is predicted by the EPR simulations. This and other possible explanations will be evaluated in future work.

Summary

While the EPR properties of the radical derived from compound **1** are not dramatically perturbed by imidazole substitution, the optical and vibrational properties are distinct when compared to an unmodified tyrosyl radical. The origin of these unique spectral properties will be explored with isotopic labeling studies. This research and future studies on the cyclic pentapeptide (including the His−phenol cross-link) alone and incorporated into a Cu-containing ligand system will provide the foundation for understanding the structural and functional properties of the cross-linked His-Tyr cofactor in cytochrome *c* oxidase.

Acknowledgment. J.A.C. and I.A. contributed equally to this work. This work was supported by National Institutes of Health Grants GM53788 (Ó.E.), GM43273 (B.A.B), and GM19541 (I.A.), the American Chemical Society Petroleum Research Fund (32051-AC1), the American Cancer Society (RGP-93-017-06-CDD), and the California Department of Health Services, Cancer Research Program (99-00632V-10129) (J.P.K). J.A.C. was supported by the Graduate Assistance in the Areas of National Need (GAANN) grant, and G.I.E. acknowledges a Roche Bioscience (Palo Alto, CA) Fellowship in synthetic organic chemistry. We thank Dr. John S. Winterle and Professors Rebecca Braslau and Eugene Switkes, Department of Chemistry and Biochemistry, University of California at Santa Cruz, for helpful discussions.

JA011852H